Dalton Transactions

Accepted Manuscript

ROYAL SOCIETY OF CHEMISTRY

www.rsc.org/dalton

A Table of Contents Entry

Title: Mesoporous Silica Nanoparticles for Enhancing Delivery Efficiency of Immunostimulatory DNA Drugs

Authors: Cuilian Tao, Yufang Zhu, Yi Xu, Min Zhu, Hiromi Morita, Nobutaka Hanagata

TOC Figure:

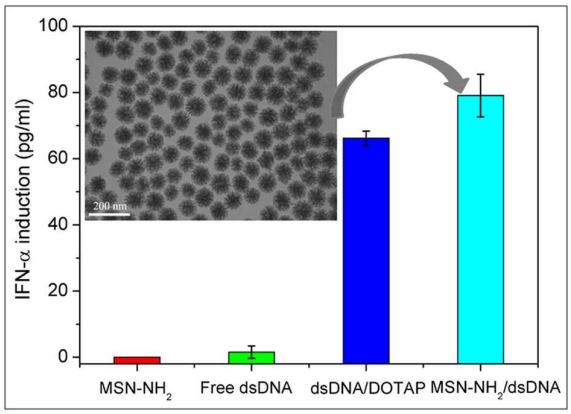

Text: A potential immunostimulatory double-stranded DNA (dsDNA) drug delivery system has been designed for enhancing the delivery efficiency.

Mesoporous Silica Nanoparticles for Enhancing Delivery Efficiency of Immunostimulatory DNA Drugs

Cuilian Tao[a], Yufang Zhu[b], Yi Xu[a], Min Zhu[b], Hiromi Morita[c], Nobutaka Hanagata[c]

[a] School of Medical Instrument and Food Engineering, University of Shanghai for Science and Technology, 516 Jungong Road, Shanghai, 200093, China.

[b] School of Materials Science and Engineering, University of Shanghai for Science and Technology, 516 Jungong Road, Shanghai, 200093, China.

[c] Nanotechnology Innovation Station, National Institute for Materials Science, 1-2-1 Sengen, Tsukuba, Ibaraki 305-0047, Japan.

*Corresponding authors: Yufang Zhu

Tel: +86-21-55271663;

Email: zjf2412@163.com

Abstract: We developed a potential immunostimulatory double-stranded DNA (dsDNA) delivery system by binding of dsDNA to amino-modified mesoporous silica nanoparticles (MSNs) to form MSN-NH_2/dsDNA complexes. Serum stability, in vitro cytotoxicity, cell uptake, and type I interferon-α (IFN-α) induction of MSN-NH_2/dsDNA complexes were evaluated. The results showed that MSN-NH_2 nanoparticles had no cytotoxicity to Raw 264.7 cells, and MSN-NH_2/dsDNA complexes enhanced serum stability of dsDNA due to the protection by nanoparticles and exhibited high efficiency of cell uptake due to small particle size and excellent dispersity. Most importantly, MSN-NH_2/dsDNA complexes significantly enhanced the level of IFN-α induction, triggered by cytosolic DNA sensor proteins. Therefore, binding of immunostimulatory DNA to MSNs would be promising for enhancing the delivery efficiency of immunostimulatory DNA drugs.

Keywords: Mesoporous silica nanoparticles, Immunostimulatory DNA, Delivery, Interferon-α

1. Introduction

Cancer is a disease caused by both a genetic predisposition and environmental factors. Chemotherapy is a common therapeutic approach, but relies on the use of cytotoxic drugs, which results in serious side-effects [1]. DNA therapy involves the delivery of a therapeutic DNA into cells, followed by stimulation and the induction of the required cytokines. It is a promising approach for the treatment or prevention of cancer because it only targets the defects that gives rise to major symptoms, and therefore avoids complications associated with chemotherapy [2-3].

DNA is a potent activator of innate immune responses in mammalian cells [4]. An efficient strategy is to deliver DNA into cells to induce type I interferons for the treatment of cancer by activation of natural killer cells [5]. Recent studies demonstrated that, in addition to the endolysosome localized Toll-like receptor 9 [6], cytosolic DNA sensors can recognize immunostimulatory DNA, and activate type I interferons (IFN) [7-11]. For example, Takaoka et al. reported that DNA triggered IFN-α/β production via cytosolic DNA sensor (Z-DNA binding protein 1) in L929 cells [7]. Yang et al. found that cytosolic nucleic acid-binding protein LRRFIP 1 binds dsDNA to induce IFN-β production in macrophages [8]. Unterholzner et al. identified that cytosolic IFI16 is an innate immune sensor in mediating an IFN-β response to intracellular DNA in THP-1, HEK293 and Raw 264.7 cells [9]. Therefore, delivering of immunostimulatory DNA into cytosol for the induction of type I interferons could be a promising approach for cancer therapy. However, clinical applications of immunostimulatory DNA as DNA drug are significantly hampered due to their nuclease degradation and rapid clearance in serum leading to limited in vivo stability

and activity [3,12].

To date, a variety of cationic nanoparticles have been developed as vehicles for DNA delivery, including polymers, lipids, polysacaccharides, peptides, and dendrimers [12-16]. Cationic vehicles are effective for in vitro delivery because they condense DNA into nanosized complexes with positive surface charge, which promotes endocytosis by electrostatically adsorbing onto anionic cell membranes [17]. However, intravenous administration of cationic lipoplexes or polyplexes often results in particle instability and nonspecific interaction with blood components that induce opsonization, aggregation of red blood cells, platelet activation, and, in extreme cases, rapid mortality [18].

Therefore, many efforts have also been made to develop inorganic nanoparticles as vehicles for DNA delivery, such as silica, Au, Fe_3O_4, quantum dots, graphene, and upconversion nanoparticles [12,19-28], which can not only efficiently protect DNA from degradation through encapsulation of DNA in their matrix or adsorption of DNA on their surface, but also promote cellular uptake via endocytosis because of their small size, and thereby increase the induction of cytokines and immune response. For example, Shi et al. reported core/shell Fe_3O_4@SiO_2 nanoparticles modified with PAH as a vector for EGFP plasmid DNA delivery into Hela cells, and found that Fe_3O_4@SiO_2/PAH nanoparticles protected the plasmid DNA from serum and DNase I degradation and demonstrated a fairly high expression level even in the presence of serum [19]. Oishi et al. used Au nanoparticles coated with SH-PEG5000-PAMA7500 and SH-siRNA, reaching a loading of 45 siRNA molecules per Au nanoparticle, and 65% knockdowm in luciferase expression in HuH-7 cells [21].

Mesoporous silica nanoparticles (MSNs) are a promising candidate carrier for drugs/DNA due to their high surface area, large pore volume, biocompatibility and ease of surface functionalization [2,29]. Recent studies also confirmed the possibility of using MSNs as a carrier for delivering nucleic acid-based drugs and other biomedical applications [2,30-40]. For example, Radu et al. reported a gene transfection system based on polyamidoamine dendrimers-modified MCM-41 nanoparticles, and the transfection efficiency was significantly enhanced compared to other commercial transfection reagents [34]. Park et al. prepared mannosylated polyethylenimine-coupled MSNs to bind plasmid DNA, and the MSNs/DNA complexes showed enhanced transfection efficiency in Raw 264.7 and HeLa cells [35]. However, most of studies designed DNA molecules to be adsorbed on the out surface of MSNs through electrostatic interaction, which result in a limited DNA loading capacity because DNA molecules could not be loaded in the mesopores [34-39].

For delivery of immunostimulatory DNA drugs, cytosolic DNA sensors recognize DNA in cytosol. Therefore, high endosomal escape capability of DNA delivery system and high level of DNA in cytosol would play an important role in enhancing the induction of type I interferons. Studies demonstrated that cell uptake and endosomal escape of MSNs are majorly dependent on the particle size [41-45]. Gan et al. investigated cell uptake and endosomal escape of MSNs with particle size from 50 to 440 nm, and found that the efficiency of cell uptake and endosomal escape strongly depended on the particle size, with the best efficiencies from 100 nm MSNs [41].Lu et al. investigated cell uptake of MSNs with particle size from 30 to 280 nm, and found that smaller MSNs exhibited higher

cell uptake ability in vitro [43]. Wang et al. reported that the RNA interference efficiency mediated by MSNs-based delivery vehicles was strongly dependent on their endosomal escape capability [44]. Therefore, MSNs with small particle size could contribute to high cell uptake ability and endosomal escape capability, and thereby enhance the immunostimulatory DNA level in cytosol. On the other hand, higher DNA loading capacity on nanoparticles is thought to be crucial factor in the enhancement of delivery efficiency [46]. Because DNA have relative large molecular size, larger pore size of MSNs could be beneficial for loading DNA in mesopores, and thereby increasing DNA loading capacity. Therefore, from viewpoint of the carrier structure, MSNs with smaller particle size and larger pore size will be better to enhance the delivery efficiency due to easy of cell uptake and endosomal escape and higher DNA loading capacity.

In this study, we report a potential immunostimulatory DNA drug delivery system based on MSNs with small particle size and large pore size. After modifying with amino groups on MSNs, dsDNA were bonded to MSNs through the electrostatic interaction to protect against degradation by nucleases. Raw 264.7 cells were used to culture with the immunostimulatory DNA delivery system, and in vitro cytotoxicity, cell uptake and the induction of IFN-α were investigated.

2. Experimental methods

2.1 Chemicals

Hexadecyltrimethylammonium p-toluenesulfonate (CTAT) and 3-aminopropyltriethoxysilane (APTES) were obtained from Sigma-Aldrich. Tetraethyl

orthosilicate (TEOS), triethanolamine (TEA), ethanol were obtained from Sinopharm Chemical Reagent Co. Ltd. Agarose I^{TM}, 6 × sucrose DNA loading buffer II, 50 × TAE buffer, ethidium bromide (EB, 10 mg/mL), fetal bovine serum (FBS), dsDNA, disodium salt dihydrate (EDTA) were obtained from Shanghai Sangon Biotech Co. Ltd. Ultrapure water was obtained from Millipore pure water system. All other chemicals were analytical-reagent grade and used without further purification.

2.2 Synthesis of mesoporous silica nanoparticles (MSNs)

MSNs were prepared according to the previously reported method with some modification [47]**.** Briefly, CTAT (0.6836 g) and TEA (4 g) were dissolved in water (36 ml) under stirring and heated at 353 K. After the surfactant was completely dissolved in water, TEOS (5.58 ml) was rapidly added to the clearly solution. The mixture was then stirred for another 2 h, resulting in the formation of a white colloidal suspension. The white particles were collected by centrifugation and washed with water and ethanol for several times, and then dried in vacuum at 333 K for 12 h. Finally, MSNs were obtained by calcining the white particles at 813K for 7 h to remove the organic templates.

2.3 Synthesis of amino-modified MSNs (MSN-NH_2)

500 mg of MSNs was homogeneously dispersed in 100 ml of ethanol by ultrasonication. And then, 1.5 ml of APTES was added to the suspension and slowly stirred the suspension for 24 h at the room temperature. The mixture was collected by centrifugation and extensively washing with ethanol to remove the residual APTES, and the obtained white particles were dried in vacuum at 333 K for 24 h.

2.4 Characterization

Scanning electron microscopy (SEM) was carried out with an FEI Quanta 450 field emission scanning electron microscope. Transmission electron microscopy (TEM) images were obtained on a Hitach-600 transmission electron microscope at an acceleration voltage of 100 kV. N_2 adsorption–desorption isotherms were obtained on a Micromeritics Tristar 3020 automated surface area and pore size analyzer at -196 ^{o}C under continuous adsorption condition. Brunauer-Emmett-Teller (BET) and Barrett-Joyner-Halenda (BJH) methods were used to determine the surface area, the pore size distribution and the pore volume. Dynamic light scattering (DLS) measurements were performed on a Malvern zeta sizer Nano-ZS90. Fourier transform infrared (FTIR) spectra were conducted on a LAM750(s) spectrometer in transmission mode. UV–vis absorption spectra were measured on a Nanodrop 2000C spectrophotometer. Thermogravimetric (TG) analysis was performed on a DMA-8000 dynamic mechanical thermal analyzer.

2.5 Binding of immunostimulatory dsDNA to MSN-NH_2 nanoparticles (MSN-NH_2/dsDNA)

The immunostimulatory dsDNA was prepared by hybridization of plus chain (5'-TCAGAGAGTTAGAGAGTTAGAGAGTCAGAGAGTTAGAGAGTTAGAGAGTCAGAGAGTTAG AGAGTTAGAGAG-3') and minus chain (5'-CTCTCTAACTCTCTAACTCTCTGACTCTCTAACTC TCTAACTCTCTGACTCTCTAACTCTCTAACTCTCTGA-3'), and the dsDNA was dissolved in ultrapure water at a concentration of 1 μg/μl and stored at -20 ^{o}C until use. To study electrostatic binding of dsDNA to MSN-NH_2 nanoparticles, MSN-NH_2 nanoparticles were suspended in ultrapure water with a concentration of 1 μg/μl. Subsequently, the as-prepared MSN-NH_2 suspension dispersed in dsDNA solution and the mixture with a weight ratio of MSN-NH_2/dsDNA = 3, 6, 12, 24, 30 or 60 was shaking at room

temperature for 4 h, respectively. Finally, MSN-NH_2/dsDNA complexes were collected by centrifugation of the mixture at 12000 rpm for 15 min. The supernatant was collected for UV-vis measurement to estimate the adsorbed dsDNA amount. The remained supernatants were analyzed with gel electrophoresis by loading onto 3% agarose gel with EB and running with loading buffer at 120 V for 30 minutes.

2.6 Stability of MSN-NH_2/dsDNA complexes

400 μg of MSN-NH_2/dsDNA complexes containing 4 μg of dsDNA was incubated in an aqueous solution containing 20% FBS at 310 K for 0, 1, 3, 5 and 7 h, respectively. After digestion, 2 μl of 250 mM EDTA was respectively added to all samples, and treated for 2 min at 353K to quench the digestion reaction. The products were collected by centrifugation and washed with water once. Finally, the as-prepared product was then analyzed with gel electrophoresis by loading onto 3% agarose gel with EB and running with loading buffer at 120 V for 30 minutes.

2.7 Cell culture

Raw 264.7 cells were purchased from InvivoGen (San Diego, CA, USA), and grown in Dulbecco's modified Eagle's medium (DMEM, Sigma-Aldrich) supplemented with 10% FBS, 50 U/ml penicillin, 50 mg/l streptomycin, 100 μg/ml normocin and 10 μg/ml blasticidin at 37 ^{o}C in humidified air containing 5 % CO_2. Raw 264.7 cells were cultured according to manufacture instructions.

2.8 In vitro cytotoxicity assay

An in vitro cytotoxicity assay for MSN-NH_2 nanoparticles was performed using a Cell Counting Kit-8 (CCK-8, Dojindo, Japan). Raw 264.7 cells were seeded in a 96-well plate at

a density of 5000 cells/well. After seeding cells, MSN-NH_2 nanoparticles solution (1 mg/ml in DMEM) was immediately added in 96-well plate. The final concentrations of MSN-NH_2 nanoparticles were 25, 50, 75, 100 and 200 μg/ml, and the final medium volume in each well was 100 μl. After incubation of cells for 24 and 48 h, 10 μl of CCK-8 solution was added in each well, and the cells were incubated for another 3 h. Absorbance at 450 nm was them measured using a microplate reader (MTP-880 Lab, Corona, Japan). Cytotoxicity was expressed as the percentage of viable cells compared with that of untreated control cells.

2.9 Cell uptake assay

Fluorescein isothiocyanate (FITC)-labeled immunostimulatory dsDNA (FITC-dsDNA) were bonded to MSN-NH_2 nanoparticles. 1.25×10^5 cells were seeded in a 35 mm glass bottom Petri dish. After incubation of cells for 24 h, MSN-NH_2 nanoparticles with or without FITC-dsDNA were added in the dish at a final concentration of 100 μg/ml. As a control, free FITC-dsDNA solution was added in the dish, and the amount was equivalent to the binding amount on MSN-NH_2 nanoparticles. When the cells had been incubated for another 24 h, they were washed twice with PBS and fixed with 3.7 % formaldehyde for 15 min. Cell nuclei were stained with Hoechst 33342 (0.5 μg/ml) for 20 min. Finally, the cells were visualized using a confocal laser scanning microscope (SP5, Laica, Germany).

2.10 Cytokine assay

Raw 264.7 cells were seeded in a 96-well plate at a density of 1×10^5 cells/well in DMEM medium. The cells were immediately stimulated with 100 μl of 0.1 mg/ml MSN-NH_2/dsDNA complexes. Free dsDNA, MSN-NH_2 nanoparticles without dsDNA and

dsDNA/DOTAP complexes (DOTAP liposomal transfection reagent, Roche Appli. Sci.) as controls were respectively added in the culture medium at the equal amounts of dsDNA or MSN-NH_2 nanoparticles in MSN-NH_2/dsDNA nanoparticles. After 48 h of incubation at 37 ^{o}C, the supernatants were collected, and the level of IFN-α in the medium was determined by an enzyme-linked immunosorbent assay (ELISA) using the human IFN-Module enzyme-linked immunosorbent assay set (eBiosciences, Vienna, Austria).

3. Results and discussion

3.1 Synthesis of MSNs and MSN-NH_2 nanoparticles

MSNs with small particle size and large pore size were synthesized using hexadecyltrimethylammonium p-toluenesulfonate as the templating surfactant and triethanolamine as the mineralizing agent according to previous reported method [47]. As shown in Fig. 1, MSNs were spherical and highly monodisperse, average particle size was about 130 nm, and mesopores also could be observed on MSNs. Particle sizes of MSNs in H_2O was further measured by dynamic light scattering (DLS) (Fig. 2). The dynamic particle sizes distribution was relatively narrow and the sizes were close to those of SEM and TEM results, which suggest the good dispersity of MSNs in aqueous solution. Studies demonstrated that cell uptake of MSNs is particle size-dependent, and smaller particle size induces high cell uptake [41]. Gan et al. reported that ca. 100 nm of MSNs exhibited the best efficiencies of cell uptake and endosomal escape in biological cells [43]. Therefore, MSNs with a particle size of 130 nm could be efficiently taken up by cells, and followed the efficient escape from endosomes into cytosol. Using N_2 physisorption

technique (Fig. 3), MSNs had a BET surface area of 625 m^2/g, the corresponding pore size distribution calculated from the desorption branch of the nitrogen isotherm by using the BJH method exhibited a bimodal pore size distribution peaked at 2.6 and 12 nm, making the possibility of dsDNA loading in the mesopores.

For binding dsDNA to MSNs, MSNs were modified with amino groups to obtain positively charged surface, which facilitate the binding of negatively charged dsDNA to MSNs through electrostatic interaction. Fig. 4 shows FTIR spectra for MSNs and MSN-NH_2 nanoparticles. After MSNs were modified with amino groups, vibration peak can be observed at 1340 and 1410 cm^{-1} assigned to the stretching bands of C-N groups. At the same time, the Si-OH band at 960 cm^{-1} in the MSNs spectrum became significantly weaker after modifying with amino groups. These results indicated that amino groups have been modified onto MSNs. Zeta potential measurements further confirmed amino modification of MSNs. As shown in Fig. 5, zeta potential of MSNs was -16.9 mV, while that of the MSN-NH_2 nanoparticles was 15.8 mV due to the modification of positively charged amino groups onto MSNs. TG analysis also confirmed the grafting of amino groups on MSNs, because the weight loss of MSN-NH_2 nanoparticles was much higher than that of MSNs (Supporting Information). On the other hand, N_2 physisorption measurements showed that the BET surface area of MSN-NH_2 nanoparticles decreased to 191 m^2/g due to the grafting of amino groups on the surface of mesopores; but the average mesopore size was still as large as 11 nm, allowing dsDNA to transport into mesopores and bind to the pore surface (Fig. 3). The amino modification of MSNs induced a slight increase in the dynamic particle size, but the particle size distribution was still narrow (Fig. 2), suggesting

that the amino modification of MSNs did not influence the dispersity in aqueous solution.

3.2 Binding and stability of dsDNA on MSN-NH_2 nanoparticles

Binding of dsDNA to MSN-NH_2 nanoparticles was confirmed using agarose gel electrophoresis, UV-vis spectra, and zeta potential measurements. As shown in Fig. 6, the dsDNA band in the supernatant can be observed at the weight ratio of MSN-NH_2/dsDNA was 3, but disappeared at a weight ratio of ≥6, which suggest that dsDNA was able to bind to MSN-NH_2 nanoparticles due to the electrostatic interaction, and at a weight ratio of 3 can be estimated to be the saturation loading of dsDNA on MSN-NH_2 nanoparticles. Determining by UV-vis analysis, the loading capacity of dsDNA on MSNs at a weight ratio of 3 was about 184 μg/mg, which was much higher than those of solid silica nanoparticles (6.7 μg/mg) and MCM-41 mesoporous silica with mesopore size of 2.5 nm (38.8 μg/mg) (Supporting Information). The higher loading capacity might be attributed to the large mesopores for dsDNA loading. On the other hand, zeta potential decreased from 15.8 mV to -12.7 mV after binding of dsDNA to MSN-NH_2 nanoparticles (Fig. 5), the characteristic adsorption peak at 260 nm for dsDNA appeared on the UV-vis spectrum of MSN-NH_2/dsDNA complexes (Fig. 7), and a little increase in dynamic particle size after binding of dsDNA to MSN-NH_2 nanoparticles (Fig. 2), also confirming that dsDNA have bonded to MSN-NH_2 nanoparticles to form MSN-NH_2/dsDNA complexes. Studies demonstrated that adsorption of DNA or siRNA on silica nanoparticles, Au nanoparticles, grapheme, magnetic nanoparticles and quantum dots increased the induction of cytokines or transfection efficiency due to the enhanced stability of DNA or siRNA [12, 19-27]. Therefore, binding of immunostimulatory dsDNA to MSN-NH_2 nanoparticles may

also enhance the dsDNA stability.

Serum stability of free dsDNA and MSN-NH_2/dsDNA was tested in 20% serum-containing medium using gel electrophoresis. As shown in Fig. 8, the dsDNA bands of MSN-NH_2/dsDNA complexes can be clearly observed in each gel well even after 7 h digestion, which indicated that MSN-NH_2/dsDNA complexes were able to protect dsDNA against degradation by nuclease. After binding of dsDNA on MSN-NH_2 nanoparticles to form MSN-NH_2/dsDNA complexes, the surrounding microenvironment could prevent enzymes to react with the phosphate groups of dsDNA. Many studies have demonstrated that inorganic nanoparticles, such as silica, Au and Fe_3O_4, can protect DNA, RNA, proteins and peptides from degradation after binding on nanoparticles [2,12,19-22]. Herein, the dsDNA bands of MSN-NH_2/dsDNA complexes were located in each gel well, which might be that MSN-NH_2/dsDNA complexes were too big to transport through the pathways of 3% agarose gel, or the applied electric field was not strong enough to drive MSN-NH_2/dsDNA complexes to move in gel. However, only after 1 h digestion, free dsDNA had no any bands on gel electrophoresis image (not shown), suggesting free dsDNA was degraded in serum-containing medium. Therefore, the higher serum stability of MSN-NH_2/dsDNA complexes would be useful for stimulating the induction of cytokines, and thereby enhancing immune response.

3.3 In vitro cytotoxicity, cell uptake and IFN-α induction of MSN-NH_2/dsDNA complexes

Investigation of the biological safety of drug/DNA delivery vehicles is critical for drug/DNA delivery. In this study, in vitro cytotoxicity of MSN-NH_2 nanoparticles to Raw 264.7 cells was evaluated using a Cell Counting Kit-8 (CCK-8) assay. As shown in Fig. 9, cell

viabilities after 24 and 48 h of incubation were similar, and no cytotoxicity was observed for MSN-NH_2 nanoparticles even at a concentration of 200 μg/ml, which suggest that MSN-NH_2 nanoparticles are safe and could be used as nonviral carrier for dsDNA delivery.

Cell uptake of dsDNA delivery system is important to enhance the induction of type I interferons and immune response, because immunostimulatory dsDNA has to be recognized by cytosolic DNA sensor proteins in cytosol after endosomal escape of dsDNA delivery system. To investigate cell uptake of MSN-NH_2/dsDNA complexes, Fluorescein isothiocyanate (FITC)-labeled dsDNA was bonded to MSN-NH_2 nanoparticles. Free FITC-dsDNA, MSN-NH_2 nanoparticles and MSN-NH_2/FITC-dsDNA complexes were incubated with Raw 264.7 cells for 4 h. As shown in Fig. 10, green fluorescence from MSN-NH_2/FITC-dsDNA complexes were distributed in the cells and primarily located between cell membrane and nucleus, which suggest that MSN-NH_2/FITC-dsDNA complexes were taken up into the endosomes after endocytosis or might have escaped from endosomes to cytosol. In contrast, for free FITC-dsDNA, no green fluorescence could be observed in the cells, indicating that free FITC-dsDNA was degraded in the culture medium or that lower cell uptake of free FITC-dsDNA made it difficult to observe the green fluorescence. On the other hand, it can not be observed any fluorescence in the cells incubated with MSN-NH_2 nanoparticles, because MSN-NH_2 nanoparticles have no chromophores. Therefore, binding of dsDNA to MSN-NH_2 nanoparticles could significantly enhance the efficiency of cell uptake of dsDNA, and thereby promote the interferon response.

To investigate the induction of cytokines by MSN-NH_2/dsDNA complexes, IFN-α

induction was evaluated using 50 μg/ml of MSN-NH_2 nanoparticles loaded with a dsDNA capacity of 100 μg/mg to stimulate Raw 264.7 cells for 48 h. For comparison, the cells were also stimulated by free dsDNA, MSN-NH_2 nanoparticles and dsDNA/DOTAP complexes with the same amounts of dsDNA or MSN-NH_2 nanoparticles. As shown in Fig. 11, free dsDNA induced very lower level of IFN-α (< 4 pg/ml) due to the poor stability of free dsDNA in culture medium, and MSN-NH_2 nanoparticles did not stimulate IFN-α induction. However, dsDNA/DOTAP and MSN-NH_2/dsDNA complexes exhibited the ability to induce much higher levels of IFN-α induction compared to free dsDNA. The IFN-α induction for dsDNA/DOTAP and MSN-NH_2/dsDNA complexes were 66.2±2.2 and 79.1±6.5 pg/ml, respectively. The results indicated that MSN-NH_2 nanoparticles could be used as carrier for dsDNA delivery and even be better than commercial DOTAP liposomal transfection reagent. One hand, MSN-NH_2 nanoparticles had higher dsDNA loading capacity, and dsDNA also can slowly release from MSN-NH_2/dsDNA complexes (supporting information). On the other hand, the formation of MSN-NH_2/dsDNA complexes enhanced cell uptake of dsDNA due to the protection by MSN-NH_2 nanoparticles as the carrier. Therefore, MSNs have potential for enhancing the delivery efficiency of immunostimulatory DNA drug and are promising as carriers for immunostimulatory DNA delivery.

4. Conclusions

In this study, a potential immunostimulatory dsDNA delivery system has been developed by binding of dsDNA to amino-modified MSNs with a particle size of 130 nm

and a mesopore size of 12 nm. MSN-NH_2 nanoparticles had a high dsDNA loading capacity (184 μg/mg) due to the contribution of large mesopores. In vitro cytotoxicity assay showed that MSN-NH_2 nanoparticles had no cytotoxicity to Raw 264.7 cells. Compared to free dsDNA, MSN-NH_2/dsDNA complexes exhibited enhanced serum stability for protecting dsDNA against degradation, and higher efficiency of cell uptake due to small particle size and excellent dispersity. Most importantly, MSN-NH_2/dsDNA complexes significantly induced higher level of IFN-α induction, and even were better than commercial DOTAP liposomal transfection reagent. Therefore, binding of immunostimulatory dsDNA to MSNs with small particle size and large pore size would be promising for enhancing the delivery efficiency of immunostimulatory dsDNA drugs.

Acknowledgment

The authors gratefully acknowledge the support by the Program for Professor of Special Appointment (Eastern Scholar) at Shanghai Institutions of Higher Learning, National Natural Science Foundation of China (No. 51102166), Program for New Century Excellent Talent in University (No. NCET-12-1053), Key Project of Chinese Ministry of Education (No. 212055), Innovation Program of Shanghai Municipal Education Commission (No. 12ZZ140), and Shanghai Shuguang Project (No. 12SG39).

References

[1] K. Nam, H. Y. Nam, P. H. Kim and S. W. Kim, *Biomaterials*, 2012, **33**, 8122-8130.

[2] C.Hom, J. Lu and F. Tamanoi, *J. Mater. Chem*. 2009, **19**, 6308–6316.

[3] W. Khan, H. Hosseinkhani, D. Ickowicz, P. D. Hong, D. S. Yu and A. J. Domb, *Acta*

Biomater. 2012, **8**, 4224-4232.

[4] S. Sharma and K. A. Fitzgerald, *PLoS Pathog.* 2011, **7,** e1001310. DOI: 10.1371/journal.ppat.1001310.

[5] E. Erikci, M. Gursel and I. Gürsel, *Biomaterials*, 2011, **32**, 1715-1723.

[6] N. Hanagata, *Inter. J. Nanomed.* 2012, *7*, 2181-2195.

[7] A. Takaoka, Z. C. Wang, M. K. Choi, H. Y. Yanai, H. Negishi, T. Ban, Y. Lu, M. Miyagishi, T. Kodama, K. Honda, Y. Ohba and T. Taniguchi, *Nature* 2007, **448**, 501-505.

[8] P. Y. Yang, H. Z. An, X. G. Liu, M. Y. Wen, Y. Y. Zheng, Y. C. Rui and X. T. Cao, *Nat. Immunol*. 2010, **11**, 487-494.

[9] L. Unterholzner, S. E. Keating, M. Baran, K. A. Horan, S. B. Jensen, S. Sharma, C. M. Sirois, T. C. Jin, T. Xiao, K. A. Fitzgerald, S. R. Paludan and A. G. Bowie, *Nat. Immunol*. 2010, **11**, 997-1004.

[10] L. Unterholzner, *Immunobiology* 2013, **218**, 1312-1321.

[11] A. Ablasser, F, Bauernfeind, G. Hartmann, E. Latz, K. A. Fitzgerald and V. Hornung, *Nat. Immunol.* 2009, **10**, 1065-1072.

[12] M. Malmsten, *Current Opinion Colloid Interface Sci*. 2013, **18**, 468-480.

[13] F. Liu, H. Qi, L. Huang and D. Liu, *Gene Therapy* 1997, **4**, 517–523.

[14] K. Regnstrom, E. G. Ragnarsson, M. Fryknas, M. Koping-Hoggard and P. Artursson, *Pharm. Res.* 2006, **23**, 475–482.

[15] R. I. Mahato, K. Anwer, F. Tagliaferri, C. Meaney, P. Leonard, M. S. Wadhwa, M. Logan, M. French and A. Rolland, *Gene Therapy* 1998, **9**, 2083–2099.

[16] S. Li, W. C. Tseng, D. B. Stolz, S. P. Wu, S. C. Watkins and L. Huang, *Gene Therapy*

1999, **6**, 585–594.

[17] M. Aleku, G. Fisch, K. Mopert, O. Keil, W. Arnold, J. Kaufmann and A. Santel , *Microvasc. Res.* 2008, **76**, 31–41.

[18] C. E. Nelson, J. R. Kintzing, A. Hanna, J. M. Shannon, M. K. Gupta and C. L. Duvall, *ACSNano*, 2013, **10**, 8870-8880.

[19] M. R. Shi, Y. Y. Liu, M. M. Xu, H. Yang, C. H. Wu and H. Miyoshi, *Macromol. Biosci*. 2011, **11**, 1563-1569.

[20] C. Kneuer, M. Sameti, U. Bakowsky, T. Schiestel, H. Schirra, H. Schmidt and C. M. Lehr, *Bioconjugate Chem.* 2000, **11**, 926-932.

[21] M. Oishi, J. Nakaogami, T. Ishii and Y. Nagasaki, *Chem. Lett*. 2006, **35**, 1046–1047.

[22] J. H. Kim, J. H. Yeom, J. J. Ko, M. S. Han, K. S. Lee, S. Y. Na and J. Y. Bae, *J. Biotechnol*. 2011, **155**, 287-292.

[23] D. Lee, K. Udaphye and P. N. Kumta, *Mater Sci Eng B* 2012, **177**, 289–302.

[24] V. V. Sokolova, I. Radtke, R. Heumann and M. Epple, *Biomaterials* 2006, **27**, 3147–53.

[25] L. Feng, S. Zhang and Z. Liu, *Nanoscale* 2011, **3**, 1252–1257.

[26] B. Chertok, A. E. David and V. C. Yang, *Biomaterials* 2011, **32**, 6245–6253.

[27] H. N. Yang, J. S. Park, D. G. Woo, S. Y. Jeon and K.-H. Park, *Biomaterials* 2012, **33**, 8670–8684.

[28] Y. Yang, F. Liu, X. Liu and B. Xing, *Nanoscale* 2013, **5**, 231–238.

[29] I. I. Slowing, J. L. Vivero-Escoto, C. W. Wu and V. S.-Y. Lin, *Adv. Drug Deliv. Rev*. 2008, **60**, 1278-1288.

[30] W. X. Mai and H. Meng, *Integrative Biology* 2013, **5**, 19-28.

[31] M. Colilla B. González and M. Vallet-Regí, *Biomater. Sci*. 2013, **1**, 114-134.

[32] Z. Li, J. C. Barnes, A. Bosoy, J. F. Stoddart and J. I. Zink, *Chem Soc. Rev*. 2012, **41**, 2590-2605.

[33] K. C.-W. Wu and Y. Yamauchi, *J. Mater. Chem*. 2012, **22**, 1251-1256.

[34] D. R. Radu, C.-Y. Lai, K. Jeftinija, E. W. Rowe, S. Jeftinija and V. S.-Y.Lin *J. Am. Chem. Soc*. 2004, **126**, 13216–13217.

[35] I. Y. Park, I. Y. Kim, M. K. Yoo, Y. J. Choi, M.-H. Cho and C. S. Cho, *Int. J. Pharm*. 2008, **359**, 280–287.

[36] H.-K. Na, M.-H. Kim, K. Park, S.-R. Ryoo, K. E. Lee, H. S. Jeon, R. Ryoo, C. B. Hyeo and D.-H. Min, *Small*, 2012, **8**, 1752-1761.

[37] A. M. Chen, M. Zhang, D. Wei, D. Stueber, O. Taratula, T. Minko and H. He, *Small* 2009, **5**, 2673–2677.

[38] E. C. Dengler, J. W. Liu, A. Kerwin, S. Torres, C. M. Olcott, B. N. Bowman, L. Armijo, K. Gentry, J. Wilkerson, J. Wallace, X. M. Jiang, E. C. Carnes, C. J. Brinker and E. D. Milligan, *J. Controlled. Release,* 2013, **168**, 209-224.

[39] A. Suwalski, H. Dabboue, A. Delalande, S. F. Bensamoun, F. Canon, P. Midoux, G. Saillant, D. Klatzmann, J. P. Salvetat and C. Pichon, *Biomaterials*, 2010, **31**, 5237-5245.

[40] X. Li, Y. J. Chen, M. Q. Wang, Y. J. Ma, W. L. Xia and H. C. Gu, *Biomaterials*, 2013, **34**, 1391-1401.

[41] Q. Gan, D. W. Dai, Y. Yuan, J. C. Qian, S. Sha, J. Ll Shi and C. S. Liu, *Biomedical Microdevices*, 2012, **14**, 259-270.

[42] E. Witasp, N. Kupferschmidt, L. Bengtsson, K. Hultenby, C. Smedman, S. Paulie, A. E .

Garcia-Bennett and B. Fadeel, *Toxic. Appl. Pharm*. 2009, **239**, 306-319.

[43] F. Lu, S.-H. Wu, Y. Hung and C.-Y. Mou, *Small*, 2009, **5**, 1408-1413.

[44] M. Q. Wang, X. Li, Y. J. Ma and H. C. Gu, *Int. J. Pharm*. 2013, **448**, 51-57.

[45] Y. S. Lin, C. P. Tsai, H. Y. Huang, C. T. Kuo, Y. Hung, D. M. Huang, Y. C. Chen and C.-Y. Mou, *Chem. Mater.* 2005, **17**, 4570-4573.

[46] Y. Manoharan, Q. M. Ji, T. Yamazaki, S. Chinnathambi, S. Chen, S. Ganesan, J. P. Hill, K. Ariga and N. Hanagata *Inter. J. Nanomed*. 2012, **7**, 3625-3635.

[47] K. Zhang, L. L. Xu, J. G. Jiang, N. Calin, K. F. Lam, S. J. Zhang, H. H. Wu, G. D. Wu, B. Albela, L. Bonneviot and P. Wu, *J. Am. Chem. Soc*. 2013, **135**, 2427-2430.

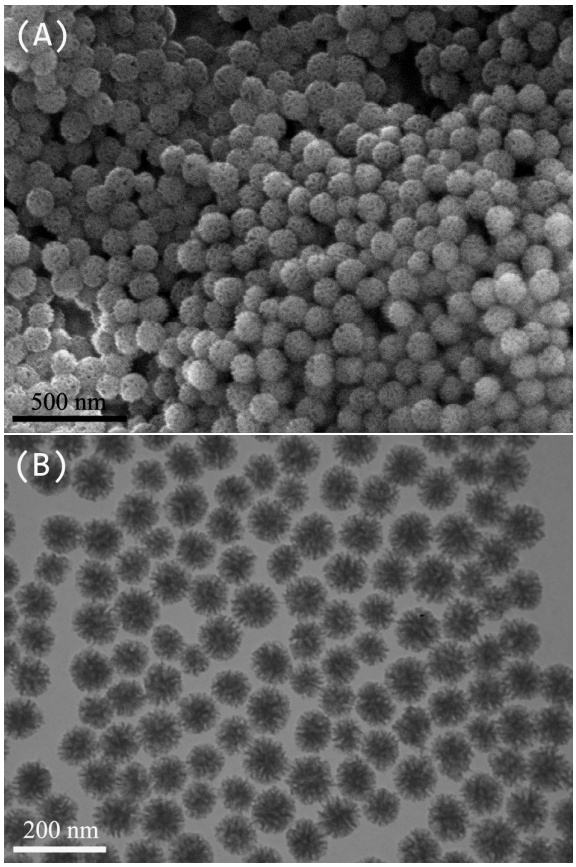

Fig. 1 SEM and TEM images of mesoporous silica nanoparticles.

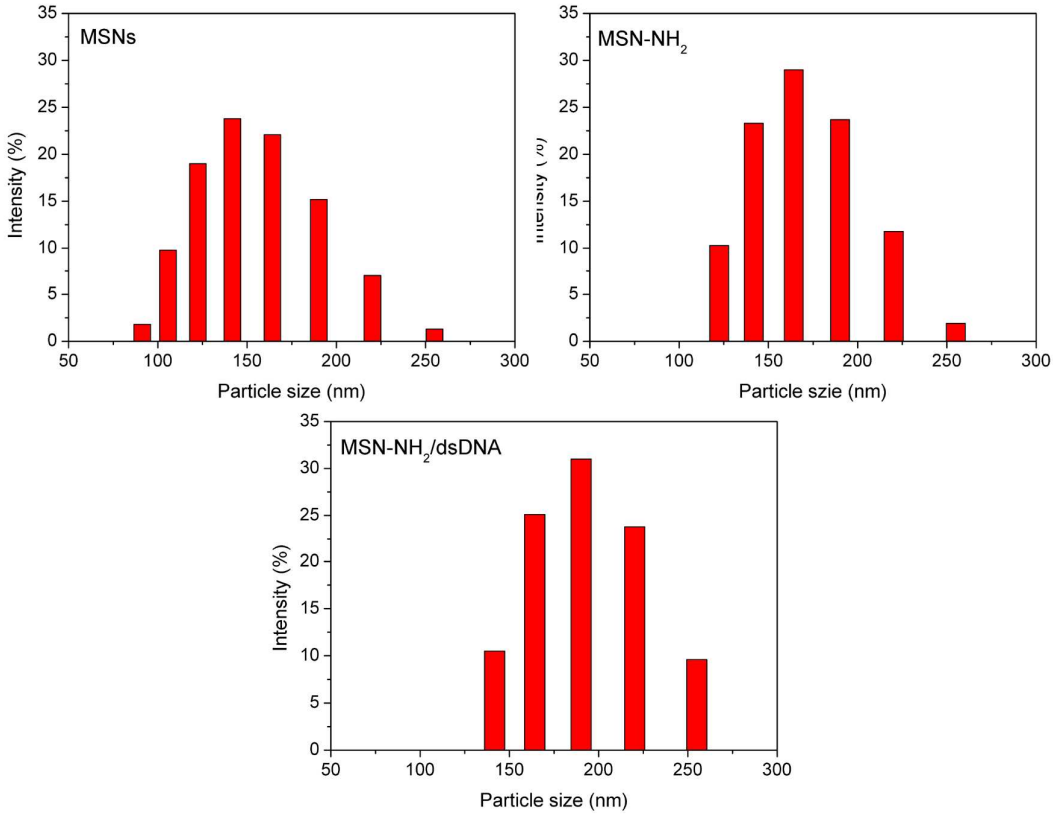

Fig. 2 Particle size distributions of the MSNs, MSN-NH_2 nanoparticles and MSN-NH_2/dsDNA complexes in H_2O, as measured by dynamic light scattering (DLS).

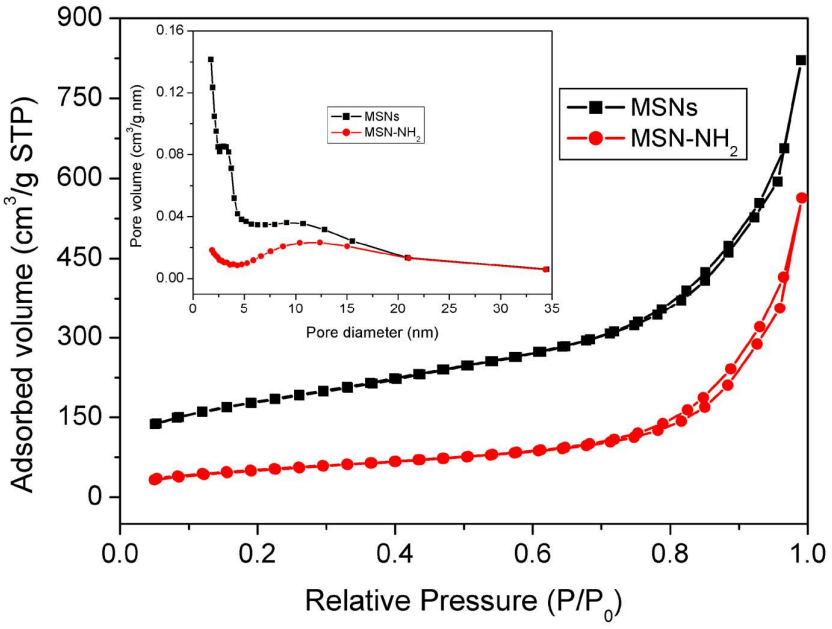

Fig. 3 N_2 adsorption-desorption isotherms and the corresponding pore size distributions of the MSNs and MSN-NH_2 nanoparticles.

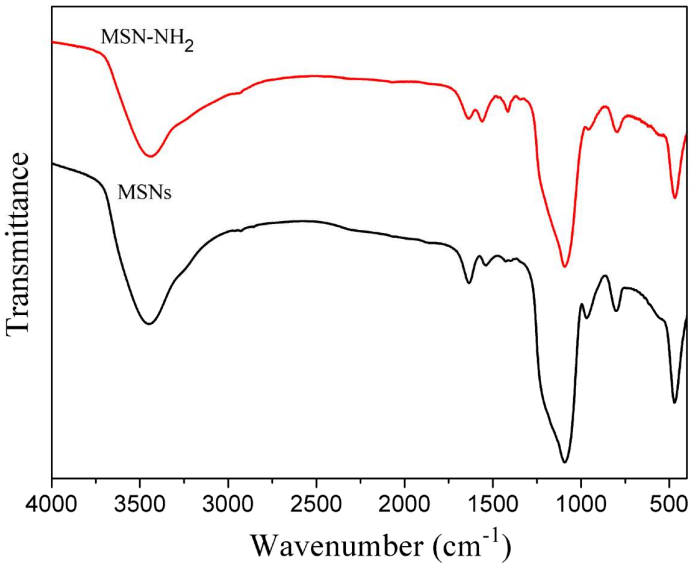

Fig. 4 FTIR spectra of the MSNs and MSN-NH_2 nanoparticles.

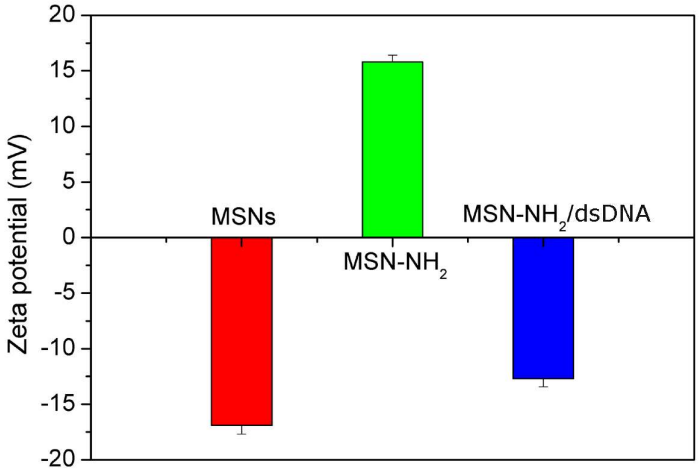

Fig. 5 Zeta potentials of the MSNs, MSN-NH_2 nanoparticles and MSN-NH_2/dsDNA complexes in PBS.

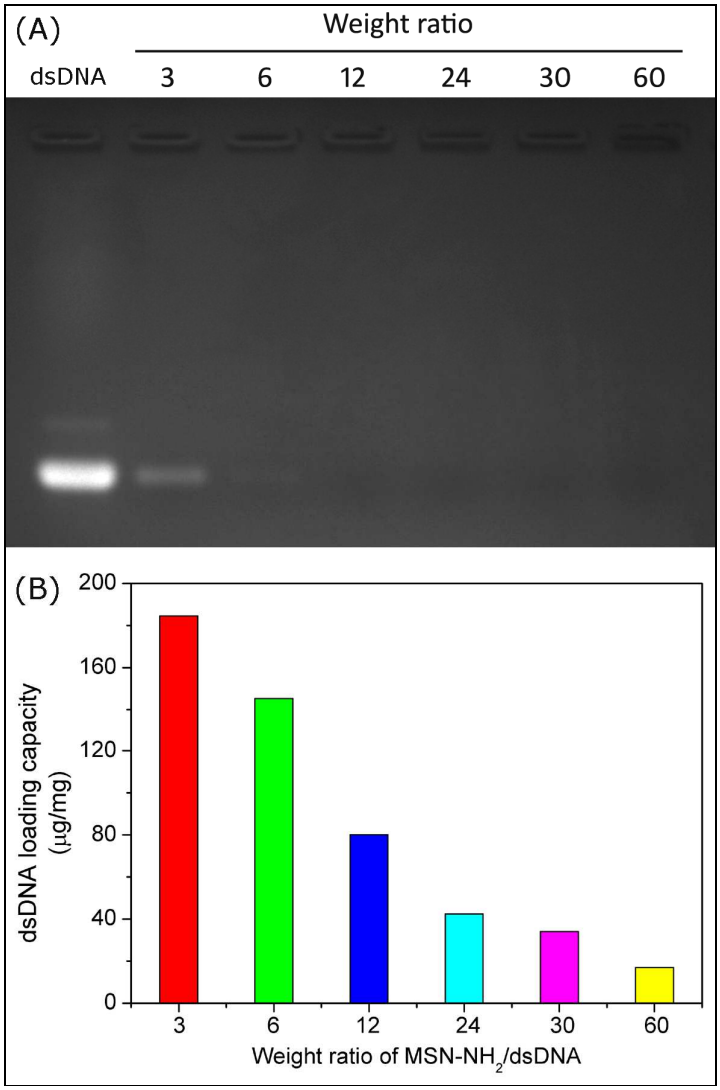

Fig. 6 (A) Agarose gel electrophoresis of the supernatants after the interaction between dsDNA and MSN-NH_2 nanoparticles at various weight ratio of MSN-NH_2/dsDNA; (B) the corresponding dsDNA loading capacities on MSN-NH_2 nanoparticles at various weight ratio of MSN-NH_2/dsDNA.

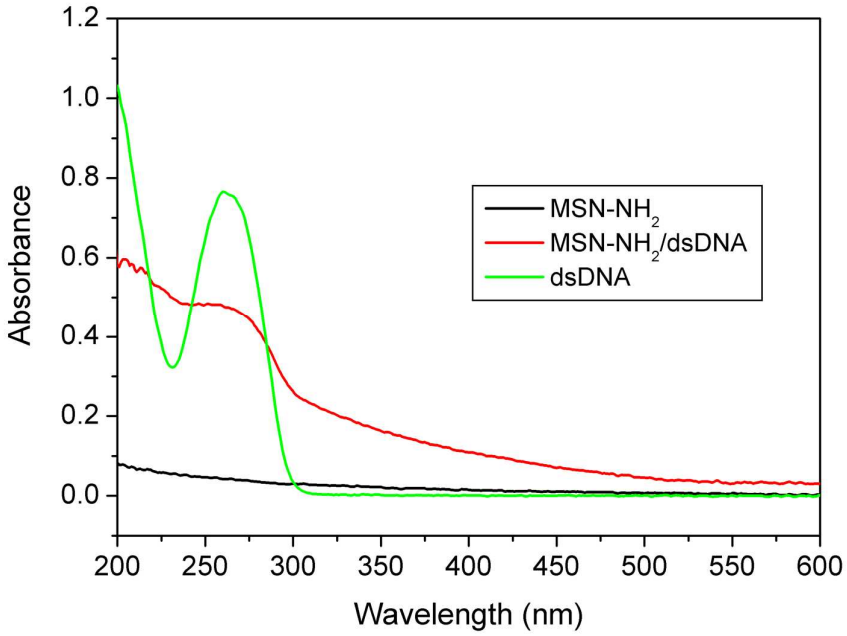

Fig. 7 UV-vis spectra of free dsDNA, MSN-NH_2 nanoparticles and MSN-NH_2/dsDNA complexes.

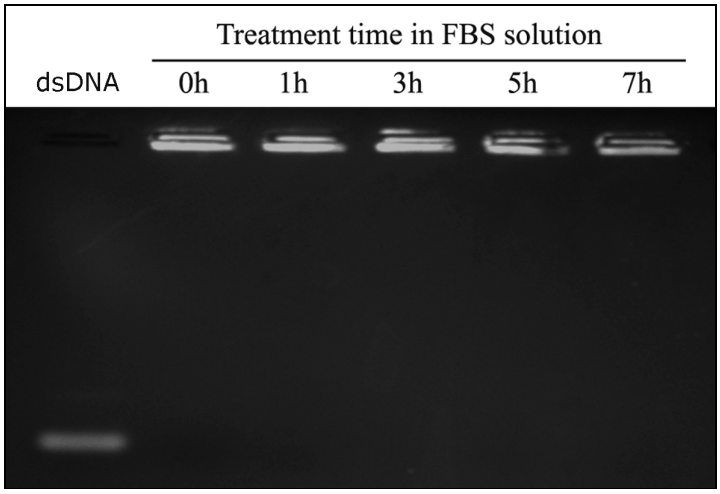

Fig. 8 Serum stability of MSN-NH_2/dsDNA complexes in 20% serum-containing media, as measured by agarose gel electrophoresis.

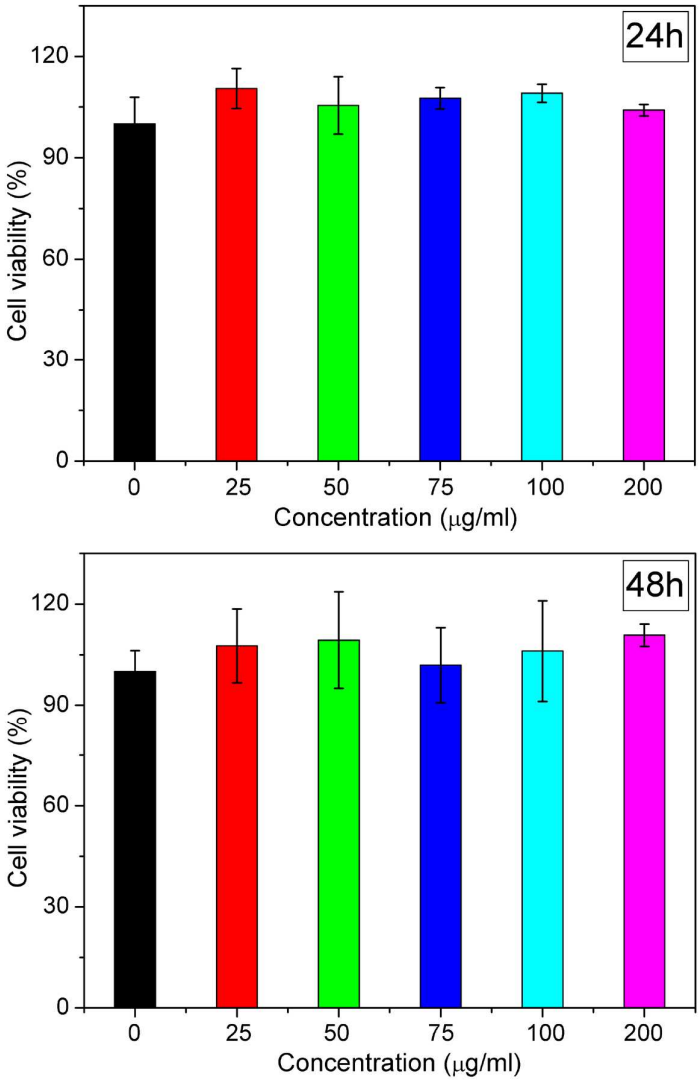

Fig. 9 Effect of the concentrations of MSN-NH_2 particles on the cytotoxicity to Raw 264.7 cells, as measured by Cell Counting Kit-8 assay.

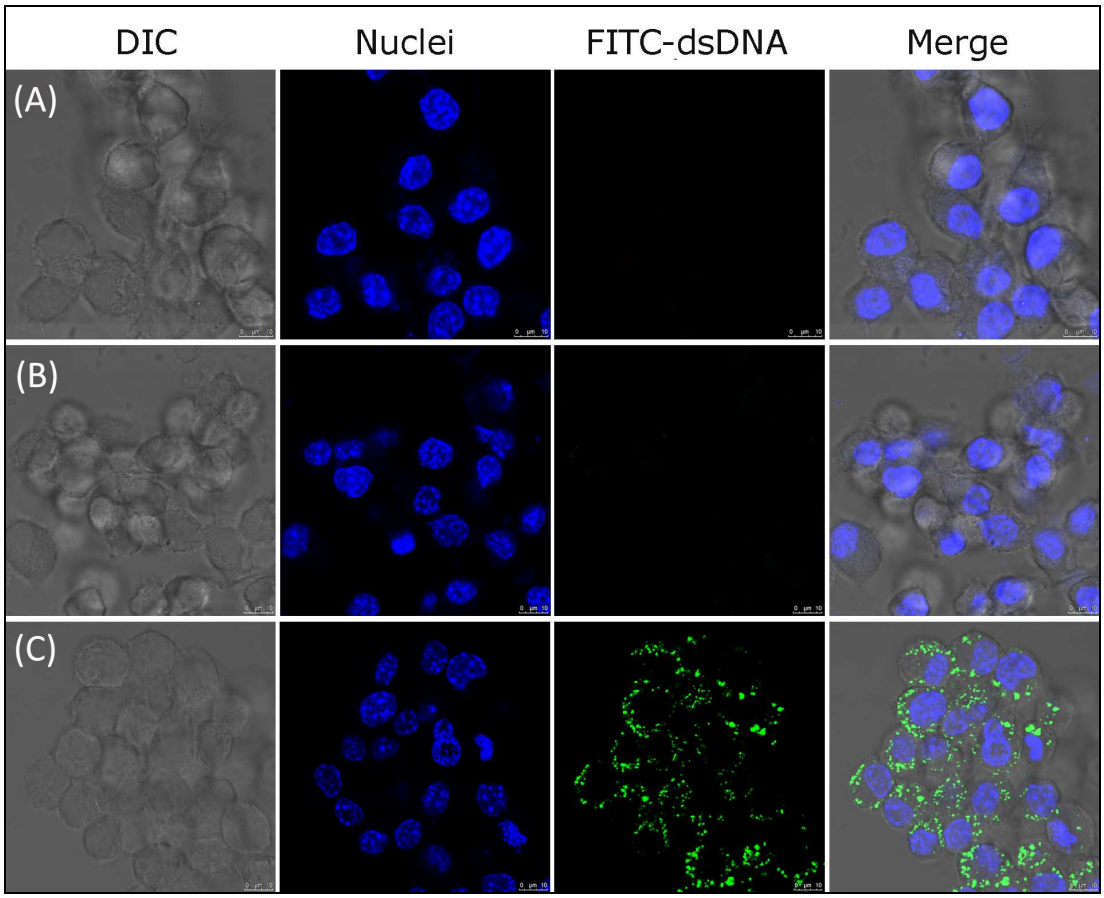

Fig. 10 Confocal microscope images of Raw 264.7 cells after 4 h incubation with MSN-NH_2 nanoparticles (A), free FITC-dsDNA (B) and MSN-NH_2/FITC-dsDNA complexes (C).

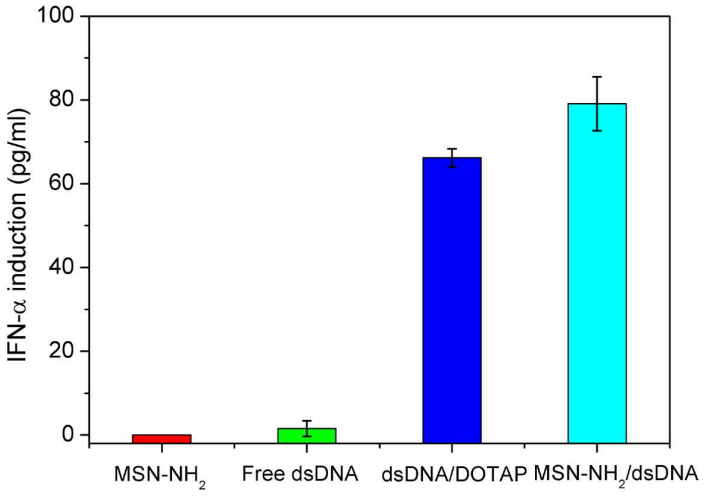

Fig. 11 INF-α induction by Raw 264.7 cells cultured with MSN-NH_2 nanoparticles, free dsDNA, dsDNA/DOTAP and MSN-NH_2/dsDNA complexes.